Pion Interferometry at RHIC: Probing a Thermalized Quark-Gluon Plasma?

Sven Soff,[1] Steffen A. Bass,[2,3] and Adrian Dumitru[4]

[1]*Physics Department, Brookhaven National Laboratory, P.O. Box 5000, Upton, New York 11973*
[2]*Department of Physics, Duke University, Durham, North Carolina 27708*
[3]*RIKEN BNL Research Center, Brookhaven National Laboratory, Upton, New York 11973*
[4]*Physics Department, Columbia University, 538 West 120th Street, New York, New York 10027*
(Received 25 December 2000)

We calculate the Gaussian radius parameters of the pion-emitting source in high-energy heavy-ion collisions, assuming a first-order phase transition from a thermalized quark-gluon plasma (QGP) to a gas of hadrons. Such a model leads to a very long-lived dissipative *hadronic* rescattering phase which dominates the properties of the two-pion correlation functions. The radii are found to depend only weakly on the thermalization time τ_i, the critical temperature T_c (and thus the latent heat), and the specific entropy of the QGP. The model calculations suggest a rapid increase of $R_{\text{out}}/R_{\text{side}}$ as a function of K_T if a thermalized QGP were formed.

Bose-Einstein correlations in multiparticle production processes [1] provide valuable information on the space-time dynamics of fundamental interactions [2]. In particular, lattice QCD calculations predict the occurrence of a phase transition at high temperature, and it is hoped that correlations of identical pions produced in high-energy collisions of heavy ions lead to a better understanding of the properties of that phase transition [for a review on quark-gluon-plasma (QGP) signatures, see [3]]. A first-order phase transition leads to a prolonged hadronization time as compared to a crossover or ideal hadron gas with no phase transition, and has been related to unusually large Hanbury-Brown–Twiss (HBT) radii [4–6]. The phase of coexisting hadrons and QGP reduces the "explosivity" of the high-density matter before hadronization, extending the emission duration of pions [4–6]. This phenomenon should then depend on the hadronization (critical) temperature T_c and the latent heat of the transition. For recent reviews on this topic we refer to [7,8].

Here we investigate if and how HBT radii, characterizing the pion source in the final state when all strong interactions have ceased, depend on the properties of the QGP and the hadronization temperature. The QGP is modeled as an ideal fluid undergoing hydrodynamic expansion with a bag model equation of state, eventually hadronizing via a first-order phase transition [6,9]. For simplicity, cylindrically symmetric transverse expansion and longitudinally boost-invariant scaling flow are assumed [6,9,10]. This approximation should be reasonable for central collisions at high energy, and around midrapidity. The model reproduces the measured p_T spectra and rapidity densities of a variety of hadrons at $\sqrt{s} = 17.4A$ GeV (CERN-SPS energy), when assuming the standard thermalization (proper) time $\tau_i = 1$ fm/c, and an entropy per net baryon ratio of $s/\rho_B = 45$ [10–12]. Because of the higher density at midrapidity, thermalization may be faster at BNL-RHIC energies—here we assume $\tau_i = 0.6$ fm/c and $s/\rho_B = 200$. (With these initial conditions, prelimi-

nary results on the multiplicity, the transverse energy, the p_T distribution of charged hadrons, and the $\overline{p}/p$ ratio at $\sqrt{s} = 130A$ GeV are described quite well [10–12]; below it will be shown that HBT correlations of pions at small relative momenta do *not* depend sensitively on these initial conditions.) The energy density and baryon density are initially distributed in the transverse plane according to a so-called "wounded nucleon" distribution with transverse radius $R_T = 6$ fm. For further details, we refer to Refs. [10–12].

We shall first discuss the radii of the $\pi^- \pi^-$ correlation functions at hadronization. From the hydrodynamical solution in the forward light cone we determine the hadronization hypersurface σ^μ. On that surface, the two-particle correlation function is given by [5,6]

$$C_2(\mathbf{p}_1, \mathbf{p}_2) = 1 + \frac{1}{\mathcal{N}} \left| \int d\sigma \cdot K e^{i\sigma \cdot q} f(u \cdot K/T) \right|^2 . \tag{1}$$

This assumes a chaotic (incoherent) and large source. f denotes a Bose distribution function. The normalization factor $\mathcal{N}$ is given by the product of the invariant single-inclusive distribution of π^- evaluated at momenta $\mathbf{p}_1$ and $\mathbf{p}_2$, respectively. u^μ denotes the four-velocity of the fluid on the hadronization surface σ^μ, and $K^\mu = (p_1^\mu + p_2^\mu)/2$, $q^\mu = p_1^\mu - p_2^\mu$ are the average four-momentum and the relative four-momentum of the pion pair, respectively. For midrapidity pions $K_\parallel = q_\parallel = 0$. Note that Eq. (1) accounts for the direct pions only but not for decays of hadronic resonances (like $\rho^0 \to \pi^+ \pi^-$, etc.), which are known to affect the correlation functions [5,7,8,13] and which will be included below.

One usually employs a coordinate system in which the *long* axis (z) is chosen parallel to the beam axis, where the *out* direction is defined to be parallel to the transverse momentum vector $\mathbf{K_T} = (\mathbf{p_{1T}} + \mathbf{p_{2T}})/2$ of the pair, and the *side* direction is perpendicular to both.

From Eq. (1), the inverse widths of the correlation function are obtained as $R_{\text{out}} = \sqrt{\ln 2}/q_{\text{out}}^*$ and $R_{\text{side}} = \sqrt{\ln 2}/q_{\text{side}}^*$ where q_{out}^*, q_{side}^* are defined by $C_2(q_{\text{out}}^*, q_{\text{side}} = 0) = C_2(q_{\text{side}}^*, q_{\text{out}} = 0) = 3/2$. Because of the definitions of the *out* and *side* directions, R_{out} probes the spatial *and* temporal extensions of the source while R_{side} probes only the spatial extension. Thus the ratio $R_{\text{out}}/R_{\text{side}}$ gives a measure of the emission duration [see also Eqs. (3)–(5) and discussion below]. It has been suggested that the ratio $R_{\text{out}}/R_{\text{side}}$ should increase strongly once the initial entropy density s_i becomes substantially larger than that of the hadronic gas at T_c [6]. Indeed, Fig. 1 shows that $R_{\text{out}}/R_{\text{side}}$ is much larger if T_c is low, such that entropy conservation dictates a long hadronization time. The closer T_c is to the initial temperature T_i (≈ 300 MeV for the BNL-RHIC initial conditions), the faster T_c is reached from above. For $(1 + 1)$-dimensional isentropic scaling expansion the time to complete hadronization is given by $\tau_H/\tau_i = s_i/s_H(T_c)$, where $s_H(T_c)$ is the entropy density of the hadronic phase at T_c. Of course, $s_H(T_c)$ increases with T_c, and so the hadronization time decreases. As R_{out} grows with the duration of pion emission [4], it must therefore decrease as T_c increases. Also, $R_{\text{out}}/R_{\text{side}}$ decreases towards large K_T as transverse flow reduces the scale of spatial homogeneity; that effect is stronger for lower T_c as transverse collective flow has more time to develop during the lifetime of the QGP.

We now proceed to include hadronic rescattering following hadronization. To describe the evolution of the hadrons towards freeze-out obviously requires one to go beyond perfect-fluid dynamics. Here we employ a semiclassical transport model that treats each particular hadronic reaction channel (formation and decay of hadronic resonance states and $2 \rightarrow n$ scattering) *explicitly* [14,15]. The transition at hadronization is performed by matching the energy-momentum tensors and conserved currents of the hydrodynamic solution and of the microscopic transport model, respectively (for details, see [12]). The microscopic
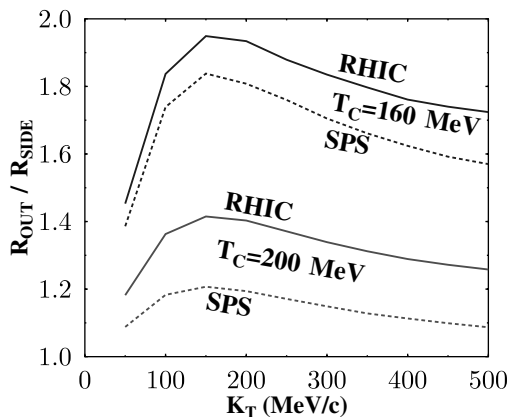

FIG. 1. Ratio of the inverse widths of the correlation function in *out* and *side* directions at hadronization, as a function of K_T; for $T_c \simeq 160$ and 200 MeV, respectively.

model propagates each individual hadron along a classical trajectory, and performs $2 \rightarrow n$ and $1 \rightarrow m$ processes stochastically. For example, the total meson-meson cross section includes a 5 mb elastic contribution as well as resonance excitation, which dominates the cross section, via

$$\sigma_{\text{res}}^{MM'}(\sqrt{s}) = \sum_{R=M^*} \langle j_M, m_M, j_{M'}, m_{M'} \| J_R, M_R \rangle$$
$$\times \frac{2S_R + 1}{(2S_M + 1)(2S_{M'} + 1)} \frac{\pi}{p_{\text{cms}}^2}$$
$$\times \frac{\Gamma_{R \rightarrow MM'} \Gamma_{\text{tot}}}{(m_R - \sqrt{s})^2 + \Gamma_{\text{tot}}^2/4} \qquad (2)$$

with the total and partial $\sqrt{s}$-dependent decay widths Γ_{tot} and $\Gamma_{R \rightarrow MM'}$. (Here $\sqrt{s}$ refers to the cm energy of the hadron-hadron scattering.) The full decay width $\Gamma_{\text{tot}}(m)$ of a resonance is defined as the sum of all partial decay widths and depends on the mass of the excited resonance. The sum extends over all resonance states which have a decay channel into MM'. The pole masses and partial decay widths are taken from [16]. The $\pi\pi$ cross section, for example, is dominated by the $\rho(770)$, with additional contributions from higher energy states. πK scattering is either elastic or proceeds through formation of mainly a $K^*(892)$ resonance. Meson-baryon elastic and resonant scattering is also taken into account. In this way, a good description of elastic and total pion cross sections *in vacuum* is obtained [15]. Collective medium-induced effects on the pion scattering [17] are neglected at present because *in a thermalized state* at $T = T_c$ there is less than one π^- per phase space cell $d^3x \, d^3p/(2\pi)^3$.

The distribution of freeze-out points of pions in the forward light cone is rather broad in time [18,19]. Freeze-out occurs in a *four-dimensional* region within the forward light cone rather than on a three-dimensional "hypersurface." The single-particle distribution of pions is not altered very much during the dissipative hadronic phase because hard collisions are rare [11,12]. (The pressure p is small, and moreover $-p \, dV$ mechanical work is largely compensated by $+T \, dS$ entropy production.) There are, however, numerous soft collisions [18], characterizing the dissipative evolution that approaches freeze-out. That means that the hadronic system, when starting from a state of local equilibrium at hadronization, disintegrates slowly rather than emitting a "flash" of pions in a rapid decay. This is fundamentally different from the "explosive" hadron production from the decay of a classical background field at the confinement transition via parametric resonance [20].

The solution of the microscopic transport provides the classical phase space distribution of the hadrons at the points of their last (strong) interaction. Bose-Einstein correlations are introduced *a posteriori* by identifying the phase space distribution at freeze-out with the Wigner density of the source [8,13,21], $S(x, K)$. Corrections arise if the pions undergo a stage of "cascading" from the

space-time point of their production to the point of their last interaction [22]. However, from the above-mentioned model for pion rescattering we find that only ~15%–20% of the pions in the final state freeze out after an elastic scattering. Rather, most pions emerge from the fragmentation of a hadronic resonance or are emitted directly from the hadronization hypersurface. Thus the source can be considered chaotic. A more detailed discussion will be given elsewhere [23].

We focus here on the so-called Gaussian radius parameters, which are obtained from a saddle-point integration over $S(x, K)$ [8,24]. The correlation functions themselves, the value of the intercept, and the effects of introducing finite momentum resolutions (as in the experimental analysis) will be discussed in [23].

The HBT-radius parameters characterizing the Gaussian *ansatz* are

$$R_{\text{side}}^2(\mathbf{K_T}) = \langle \tilde{y}^2 \rangle (\mathbf{K_T}), \tag{3}$$

$$R_{\text{out}}^2(\mathbf{K_T}) = \langle (\tilde{x} - \beta_t \tilde{t})^2 \rangle (\mathbf{K_T})$$
$$= \langle \tilde{x}^2 + \beta_t^2 \tilde{t}^2 - 2\beta_t \tilde{x}\tilde{t} \rangle (\mathbf{K_T}), \tag{4}$$

$$R_{\text{long}}^2(\mathbf{K_T}) = \langle (\tilde{z} - \beta_l \tilde{t})^2 \rangle (\mathbf{K_T}), \tag{5}$$

with $\tilde{x}^\mu(\mathbf{K_T}) = x^\mu - \langle x^\mu \rangle (\mathbf{K_T})$ being the space-time coordinates relative to the momentum dependent *effective source centers*. The average in (3)–(5) is taken over the emission function, i.e., $\langle f \rangle (K) = \int d^4x \, f(x) S(x, K) / \int d^4x \, S(x, K)$. In the *osl* system $\boldsymbol{\beta} = (\beta_t, 0, \beta_l)$, where $\boldsymbol{\beta} = \mathbf{K}/E_K$ and $E_K = \sqrt{m^2 + \mathbf{K}^2}$. Below, we shall cut on midrapidity pions ($\beta_l \sim 0$); thus the radii are obtained in the *longitudinally comoving frame*. In the absence of $\tilde{x}$-$\tilde{t}$ correlations, a large duration of emission $\Delta\tau = \sqrt{\langle \tilde{t}^2 \rangle}$ increases R_{out} relative to R_{side} [4–6].

Figure 2 shows the HBT radii and $\Delta\tau$. Also, we have varied the bag parameter B from 380 to 720 MeV/fm³, corresponding to critical temperatures of $T_c \simeq 160$ MeV and $T_c \simeq 200$ MeV, respectively. Note that within the bag model this automatically corresponds to a large variation of the latent heat ~$4B$ as well, serving the purpose of proving the (in)sensitivity of the HBT radii to variations of the phase transition parameters in this model. We also note that changing T_c implies variation of the longitudinal and transverse flow profile on the hadronization hypersurface (which is the initial condition for the subsequent hadronic rescattering stage) over a broad range.

It is obvious from Fig. 2 that the HBT radii are rather similar for all cases considered. They depend only weakly on the specific entropy, on the critical temperature and latent heat for the transition, on the thermalization time τ_i, or on the initial condition for the hadronic rescattering stage. Thus, the properties of the QGP phase are not directly reflected in the HBT radii, which are essentially determined by the large space-time volume of the hadronic rescattering stage. Soft hadronic scattering occurs over a
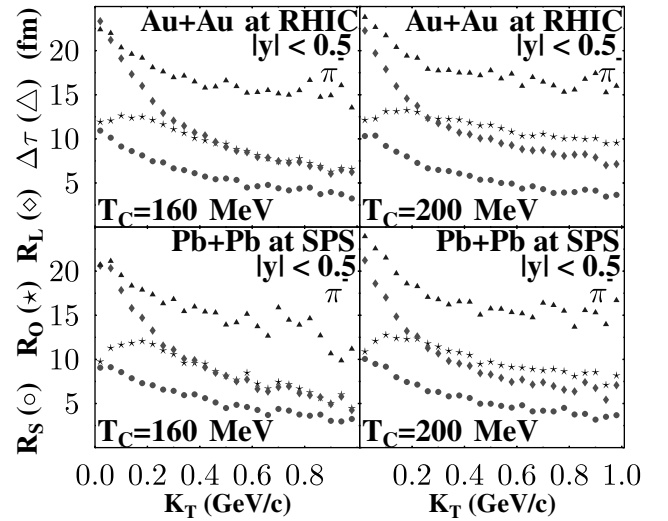

FIG. 2. HBT radii R_{out} R_{side}, R_{long}, and emission duration $\Delta\tau$ at freeze-out as a function of K_T; for central collisions at RHIC (above) and SPS (below) and $T_c \simeq 160$ MeV (left) and $T_c \simeq 200$ MeV (right).

long time span after hadronization [18], and therefore the pion mean free path increases gradually towards freeze-out [25]. Pions are emitted over a broad time interval and from the entire volume. Hence, the emission duration is large; see Fig. 2.

In Fig. 3 we compare $R_{\text{out}}/R_{\text{side}}$ at hadronization to that at freeze-out. Clearly, up to $K_T \sim 200$ MeV, $R_{\text{out}}/R_{\text{side}}$ is independent of T_c, or $s_H(T_c)$, if hadronic rescatterings are taken into account. Moreover, at higher K_T the dependence on T_c is even reversed: for high T_c the $R_{\text{out}}/R_{\text{side}}$ ratio even exceeds that for low T_c. Higher T_c speeds up hadronization but, on the other hand, prolongs the dissipative hadronic phase that dominates the HBT radii. This is because during the nonideal hadronic expansion the scale of spatial homogeneity of the pion density distribution increases, as the pions fly away from the center, but the
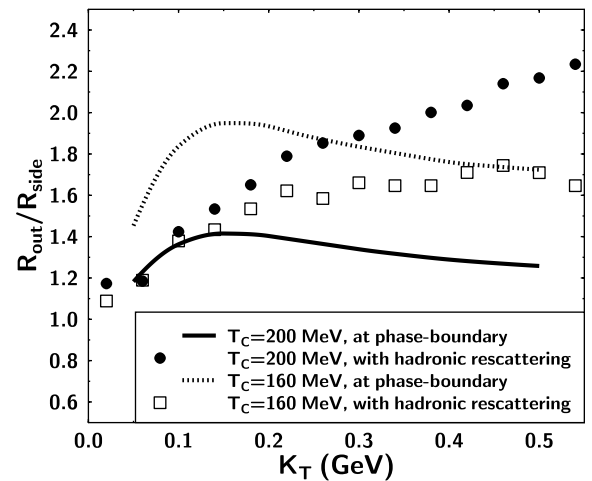

FIG. 3. $R_{\text{out}}/R_{\text{side}}$ for RHIC initial conditions, as a function of K_T at freeze-out (symbols) and at hadronization (lines).

transverse flow can hardly increase to counteract (similar to a Hubble expansion at small pressure). Therefore, after hadronic rescattering R_{out}/R_{side} does not drop towards higher K_T (in the range $K_T \lesssim 3m_\pi$).

Experimental data [26,27] for central Pb + Pb collisions at $\sqrt{s} = 17.4A$ GeV indicate smaller HBT radii than seen in Fig. 2, in particular at $K_T \leq 100$ MeV. All three radii are ≤ 10 fm. One should keep in mind, though, that experimental uncertainties are largest at small K_T, where also Coulomb, acceptance, and efficiency corrections are largest and experimental momentum resolution effects are crucial. At $K_T > 200$ MeV, the calculated HBT radii agree better with data. The experimental momentum resolution or the fit procedures could in effect reduce the extracted radii—these rather technical issues will be investigated in a detailed forthcoming study [23]. On the other hand, our calculation gives a similar K_T dependence of the three radii as seen in the SPS data: a strong decrease of R_{long}, a weaker decrease of R_{side}, and rather flat behavior of R_{out} with K_T. Most striking is that a new preliminary NA49 data analysis [27] shows a rising R_{out}/R_{side} ratio, rather similar to our results for the SPS energy with $T_c \simeq 160$ MeV [23].

Nevertheless, good agreement with the data might not be possible to achieve for R_{out} and R_{long}. That would point at too large duration of emission, $\Delta\tau$, and too large spatial homogeneity scale in this model scenario of a first-order phase transition from a thermalized QGP to a hadron gas phase. Note that single-particle spectra above $p_T \sim m_\pi$ are described quite well [10–12]. This emphasizes the importance of interferometry as a crucial test of the QGP model with hadronization through a mixed phase, as HBT probes the small momentum transfer dynamics and the spatial homogeneity scale at freeze-out.

At the higher RHIC energy, the model can be tested at even higher K_T, where experimental resolutions and corrections will be less of an issue. Also, higher energy densities will be achieved, such that the QGP model should in principle be more reliable. For central collisions of Au nuclei at $\sqrt{s} = 130A$ GeV, preliminary data from STAR gives $R_{out}/R_{side} \simeq 1.1$ at small K_T [28]. Results from RHIC at higher K_T will test whether a long-lived *hadronic* soft-rescattering stage, associated with the formation and hadronization of an equilibrated QGP state is indeed seen in heavy-ion collisions at the highest presently attainable energies.

[1] G. Goldhaber, S. Goldhaber, W. Lee, and A. Pais, Phys. Rev. **120**, 300 (1960).

[2] E. Shuryak, Phys. Lett. **44B**, 387 (1973); M. Gyulassy, S. K. Kauffmann, and L. W. Wilson, Phys. Rev. C **20**, 2267 (1979); A. Makhlin and Y. Sinyukov, Z. Phys. C **39**, 69 (1988); Y. Hama and S. S. Padula, Phys. Rev. D **37**, 3237 (1988).

[3] S. A. Bass, M. Gyulassy, H. Stöcker, and W. Greiner, J. Phys. G **25**, R1 (1999).

[4] S. Pratt, Phys. Rev. D **33**, 1314 (1986); G. Bertsch, M. Gong, and M. Tohyama, Phys. Rev. C **37**, 1896 (1988); G. Bertsch, Nucl. Phys. **A498**, 173c (1989).

[5] B. R. Schlei, U. Ornik, M. Plümer, and R. M. Weiner, Phys. Lett. B **293**, 275 (1992); J. Bolz, U. Ornik, M. Plümer, B. R. Schlei, and R. M. Weiner, Phys. Rev. D **47**, 3860 (1993).

[6] D. Rischke and M. Gyulassy, Nucl. Phys. **A608**, 479 (1996).

[7] R. M. Weiner, Phys. Rep. **327**, 249 (2000); T. Csörgő, hep-ph/0001233.

[8] U. Wiedemann and U. Heinz, Phys. Rep. **319**, 145 (1999).

[9] H. von Gersdorff, L. McLerran, M. Kataja, and P. V. Ruuskanen, Phys. Rev. D **34**, 794 (1986); **34**, 2755 (1986).

[10] A. Dumitru and D. Rischke, Phys. Rev. C **59**, 354 (1999).

[11] A. Dumitru, S. A. Bass, M. Bleicher, H. Stöcker, and W. Greiner, Phys. Lett. B **460**, 411 (1999).

[12] S. A. Bass and A. Dumitru, Phys. Rev. C **61**, 064909 (2000).

[13] M. Gyulassy and S. Padula, Phys. Lett. B **217**, 181 (1989).

[14] S. A. Bass et al., Prog. Part. Nucl. Phys. **41**, 255 (1998).

[15] M. Bleicher et al., J. Phys. G **25**, 1859 (1999).

[16] Review of Particle Physics, Eur. Phys. J. C **3**, 1 (1998).

[17] M. Gyulassy and W. Greiner, Ann. Phys. (N.Y.) **109**, 485 (1977); A. B. Migdal, Rev. Mod. Phys. **50**, 107 (1978); G. E. Brown, V. Koch, and M. Rho, Nucl. Phys. **A535**, 701 (1991).

[18] S. A. Bass et al., Phys. Rev. C **60**, 021902 (1999).

[19] L. V. Bravina, I. N. Mishustin, N. S. Amelin, J. P. Bondorf, and L. P. Csernai, Phys. Lett. B **354**, 196 (1995); H. Sorge, Phys. Lett. B **373**, 16 (1996); S. Pratt and J. Murray, Phys. Rev. C **57**, 1907 (1998).

[20] R. D. Pisarski, Phys. Rev. D **62**, 111501 (2000); A. Dumitru and R. D. Pisarski, hep-ph/0010083.

[21] S. Pratt, T. Csörgő, and J. Zimanyi, Phys. Rev. C **42**, 2646 (1990).

[22] S. S. Padula, M. Gyulassy, and S. Gavin, Nucl. Phys. **B329**, 357 (1990); A. Makhlin and E. Surdutovich, Phys. Rev. C **59**, 2761 (1999).

[23] S. Soff, S. A. Bass, and A. Dumitru (to be published).

[24] S. Chapman, J. R. Nix, and U. Heinz, Phys. Rev. C **52**, 2694 (1995).

[25] M. Prakash, M. Prakash, R. Venugopalan, and G. Welke, Phys. Rep. **227**, 321 (1993).

[26] NA49 Collaboration, H. Appelshäuser et al., Eur. Phys. J. C **2**, 661 (1998); NA44 Collaboration, I. G. Bearden et al., Nucl. Phys. **A661**, 456 (1999); WA98 Collaboration, M. M. Aggarwal et al., Eur. Phys. J. C **16**, 445 (2000).

[27] C. Blume, in Proceedings of Quark Matter 2001, Stony Brook, NY (to be published).

[28] J. Harris, F. Laue, and S. Panitkin, in Proceedings of Quark Matter 2001, Stony Brook, NY (to be published).